The Evolution of Photosynthetic Anatomy in *Viburnum* (Adoxaceae)
Author(s): David S. Chatelet, Wendy L. Clement, Lawren Sack, Michael J. Donoghue, and Erika J. Edwards
Source: *International Journal of Plant Sciences*, Vol. 174, No. 9 (November/December 2013), pp. 1277-1291
Published by: The University of Chicago Press
Stable URL: http://www.jstor.org/stable/10.1086/673241
Accessed: 19/11/2013 11:25

Int. J. Plant Sci. 174(9):1277–1291. 2013.

1058-5893/2013/17409-0007$15.00 DOI: 10.1086/673241

THE EVOLUTION OF PHOTOSYNTHETIC ANATOMY IN *VIBURNUM* (ADOXACEAE)

David S. Chatelet,[1,*] Wendy L. Clement,† Lawren Sack,‡ Michael J. Donoghue,§ and Erika J. Edwards*

*Department of Ecology and Evolutionary Biology, Brown University, Box G-W, 80 Waterman Street, Providence, Rhode Island 02912, USA; †Department of Biology, College of New Jersey, 2000 Pennington Road, Ewing, New Jersey 08628, USA; ‡Department of Ecology and Evolutionary Biology, University of California, 621 Charles E. Young Drive South, Los Angeles, California 90095, USA; and §Department of Ecology and Evolutionary Biology, Yale University, P.O. Box 208106, New Haven, Connecticut 10620, USA

Editor: Adrienne Nicotra

Premise of research. Leaf mesophyll is often differentiated into a palisade layer with tightly packed, elongated cells (I-cells) and a spongy layer with loosely packed, complex shaped cells. An alternative palisade type, composed of branched H-cells, has evolved in a number of plant lineages. *Viburnum* (Adoxaceae) possesses both types of palisade, providing an opportunity to assess the significance of evolutionary switches between these forms.

Methodology. An anatomical survey of 80 species spanning the *Viburnum* phylogeny permitted an analysis of palisade differences in relation to other characters. A geometric model of leaf mesophyll surface area for CO_2 absorption correlated well with measured photosynthetic capacity in a subset of species, allowing us to infer shifts in photosynthetic function.

Pivotal results. Ancestrally, viburnums probably produced a palisade with one layer of H-cells. Multiple transitions to two layers of H-cells (H2) and to one or two layers of I-cells (I1, I2) occurred. These shifts were correlated with increases in photosynthetic capacity, and H2 appear functionally equivalent to I1 with respect to CO_2 absorption.

Conclusions. Photosynthetic anatomy H2 and I1 palisade may represent alternative evolutionary solutions for increasing leaf CO_2 absorption. Additionally, H-cells and I-cells might perform differently with respect to light absorption and/or drought tolerance. The evolution of I-palisade cells may thus have tracked movements into open environments, while H2 could increase photosynthetic capacity in the forest understory.

Keywords: Viburnum, mesophyll, palisade, H-cell, photosynthesis, evolution.

Online enhancements: appendix figure, supplementary table.

Introduction

Leaves are specialized organs that intercept light and absorb CO_2 for photosynthesis. These functions are facilitated by specialization of the internal tissue, which is typically divided into the palisade mesophyll and the spongy mesophyll. The palisade mesophyll is generally characterized by tightly packed elongated cells just beneath the adaxial epidermis. The spongy mesophyll is composed of complex shaped, loosely packed cells typically located above the abaxial epidermis. The specialized structure of both layers aids in efficient capture of light and CO_2. Because light typically enters the leaf adaxially, the cells of the palisade layer, with their elongated shape, channel excess direct irradiance into the spongy mesophyll (Vogelmann and Martin 1993; Vogelmann et al. 1996). The elongate shape of the palisade mesophyll also provides high cell surface area relative to volume, which benefits CO_2 diffusion into palisade chloroplasts (Turrell 1936). In turn, the complex shaped cells of the spongy mesophyll serve to scatter light throughout the leaf, maximizing absorption (Terashima and Evans 1988; DeLucia et al. 1996; Evans et al. 2004; Johnson et al. 2005). Because stomata are mostly concentrated on the abaxial surface, the spongy mesophyll, with its network of large intercellular air spaces, also facilitates the diffusion of CO_2 throughout the leaf.

This typical organization of leaf tissues, especially the presence of elongate palisade cells, has been considered as optimal, but some species manifest a strikingly distinct type of palisade consisting of irregularly shaped cells. Haberlandt (1884) referred to this palisade type as arm-palisade, composed of what he termed arm-cells or H-cells (we use the latter term throughout) owing to their characteristically branched shape. Instead of being elongated, these cells appear shorter and, as their name indicates, they have lobes or arms directed toward the adaxial epidermis and sometimes also toward the spongy mesophyll. Haberlandt (1884) reported arm-palisade (hereafter, H-palisade) in some ferns, conifers, and a number of distantly

[1] Author for correspondence; e-mail: david_chatelet@brown.edu.

Manuscript received February 2013; revised manuscript received May 2013; electronically published October 14, 2013.

related angiosperms (e.g., *Viburnum* and *Sambucus* in Dipsacales, *Aconitum* in Ranunculales).

Why have species evolved different forms of palisade tissue? Do the different forms scale up to differences in higher-level function? Previous studies have largely been descriptive (Chonan 1970; Harris 1971; Campbell 1972), and although several hypotheses have been proposed, to the best of our knowledge these have not been tested. The oldest ideas were offered by G. Haberlandt in *Physiological Plant Anatomy* (1884; http://archive.org/details/physiologicalpla00habeuoft). Haberlandt developed two different hypotheses. Early in his treatment, he presented the two different palisade types as an example of functional equivalence, proposing that the two forms were equally effective outcomes of selection for a palisade layer. Later in his text, Haberlandt analyzed the two types from the standpoint of cell surface area for a given volume of tissue, and he reasoned that greater surface area would provide greater exposure of the chloroplasts to CO_2 and hence greater photosynthetic capacity. He concluded that in this regard, unbranched, elongated cells (hereafter, I-cells) would have an advantage over even deeply invaginated H-cells. Alternatively or additionally, invaginations could provide greater mechanical strength (Reinhard 1905; Meyer 1962) or facilitate CO_2 diffusion in the palisade owing to the air spaces created by the invaginations (Wiebe and Al-Saadi 1976). However, to date, functional comparisons between H-cells and I-cells have not been made.

We focused on *Viburnum* (Adoxaceae) as an ideal system for examining the evolution of photosynthetic anatomy. As previously noted by Haberlandt, *Viburnum* contains species with H-cells, but the lineage also includes many species that have typical I-cells. *Viburnum* consists of ~170 species found mainly in temperate forests of the Northern Hemisphere but also in tropical forests in Southeast Asia and in montane cloud forests throughout Central and South America. Given the relatively detailed current phylogenetic knowledge for *Viburnum* (e.g., Clement and Donoghue 2011, 2012) and its exceptional diversity in leaf traits (Schmerler et al. 2012; Weber et al. 2012), the group provides an excellent opportunity to tease apart the functional consequences of different palisade types. Here we document the diversity of palisade forms in *Viburnum* and demonstrate a striking phylogenetic pattern in the distribution of the different forms. We inferred where evolutionary shifts in palisade anatomy have occurred and tested for correlated changes in relevant morphological and environmental characteristics. Using direct measurements of photosynthesis and a CO_2 absorption model based on cell dimensions, we also tested whether evolutionary shifts in palisade anatomy were correlated with changes in photosynthetic capacity.

Material and Methods

Viburnum *Phylogeny*

For this study, we focused on a subset of the *Viburnum* species from Clement and Donoghue (2011) along with 15 newly sequenced taxa (app. A), for a total of 86 tips representing 80 species. Notable additions include six species from the *Succodontotinus* clade and four Southeast Asian species representing the *Coriacea* and *Sambucina* clades (classification following Clement and Donoghue 2011). Total genomic DNA was extracted using a Qiagen DNeasy kit, following the manufacturer's protocol, from leaf tissue either dried in silica or sampled from herbarium specimens (app. A). Following the methods of Clement and Donoghue (2011), 10 gene regions, including nine chloroplast regions (*mat*K, *ndh*F, *pet*B-*pet*D, *rbc*L, *rpl*32-*trn*L, *trn*C-*ycf*6, *trn*G-*trn*S, *trn*H-*psb*A, *trn*K) and the nuclear ribosomal internal transcribed spacer region (ITS), were amplified and sequenced.

For phylogenetic analyses, the data were divided among three partitions: (1) chloroplast coding regions (*rbc*L, *ndh*F, and *mat*K), (2) chloroplast noncoding intergenic spacer regions (*pet*B-*pet*D, *rpl*32-*trn*L, *trn*C-*ycf*6, *trn*G-*trn*S, *trn*H-*psb*A, *trn*K), and (3) ITS. Each partition was unlinked in the analysis and allowed to run under its own model of sequence evolution selected using jModeltest (Guindon and Gascuel 2003; Darriba et al. 2012) and the Akaike Information Criterion. On the basis of previous analyses (e.g., Clement and Donoghue 2011), the tree was rooted along the *Viburnum clemensiae* branch. The data were analyzed with MrBayes (ver. 3.2.1; Huelsenbeck and Ronquist 2001) running six chains for 40 million generations and sampled every 1000 generations. All parameters were visually evaluated using Tracer (ver. 1.5; Rambaut and Drummond 2007) to assure that they had reached stationarity at the conclusion of the run. The first 10% of the trees were removed before summarizing parameters and tree statistics using the sump and sumt commands within MrBayes. Trees sampled from the posterior distribution were summarized using a 50% majority consensus.

Plants for Anatomical Studies

Five mature leaves from each of 86 accessions were collected from living plants at multiple sites around the world (table B1, available online). In the United States, these sites included the Arnold Arboretum of Harvard University (Jamaica Plain, MA), the Washington Park Arboretum (Seattle, WA), and the Harvard Forest (St. Petersham, MA). Other sites were located in Mexico, Panama, Costa Rica, Malaysia, Vietnam, Taiwan, and Japan.

Gas Exchange Measurements

Light-saturated leaf photosynthetic rate per unit leaf area (A_{max}) was measured on 36 *Viburnum* taxa in a common garden at the Arnold Arboretum during the summers of 2009 and 2010. All *Viburnum* taxa with at least two individuals were studied, and A_{max} was measured on five fully expanded leaves from two to three individuals each, using a portable photosynthesis system (Li-6400; Li-Cor, Lincoln, NE). Measurements were made on sun-exposed leaves between 10:00 a.m. and 2:00 p.m. at a photosynthetically active radiation of 1500 μmol m^{-2} s^{-1}, a target temperature of 22°C, a CO_2 partial pressure of 400 ppm, and a relative humidity between 30% and 50%.

Leaf Anatomy

For each species, mature leaves were collected and fixed in either ethanol or the standard formalin–acetic acid–alcohol fixative solution. Three leaf sections of ~5 mm × 3 mm were

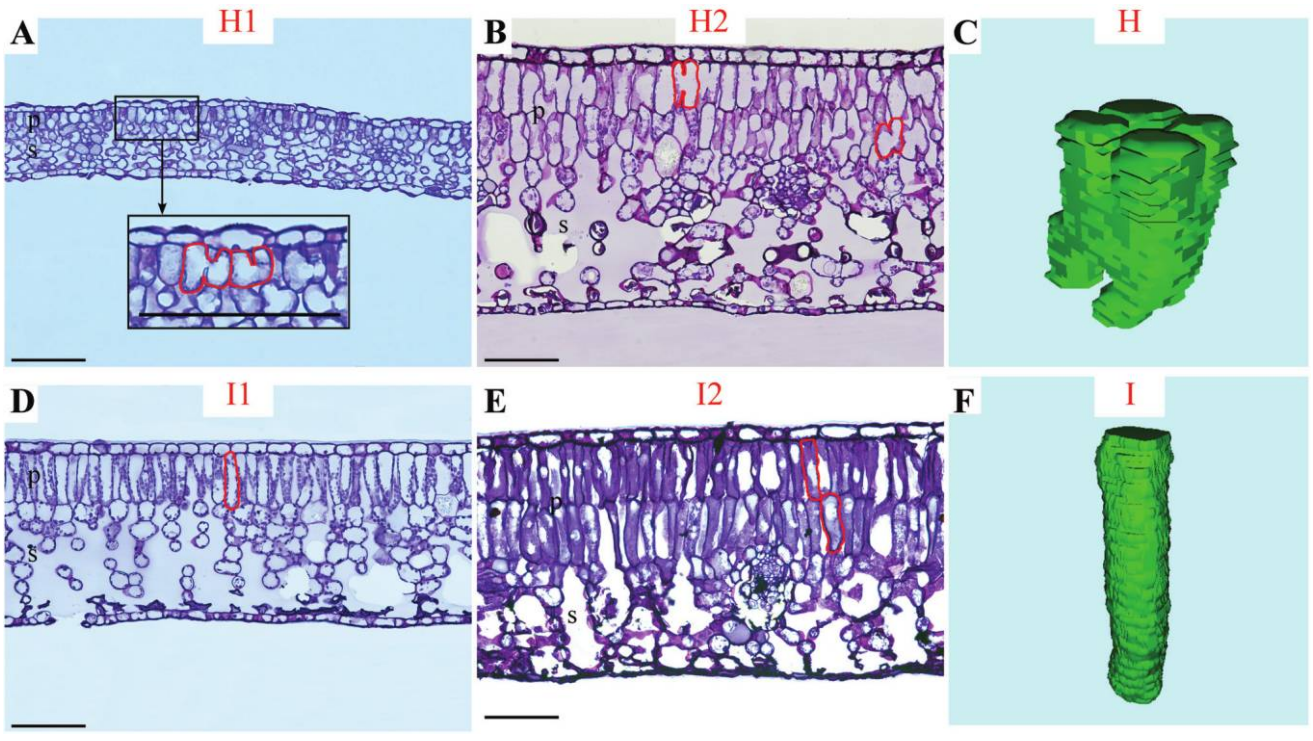

Fig. 1 Leaf palisade cell types. *A*, One layer of H-cells. *B*, Two layers of H-cells. *D*, One layer of I-cells. *E*, Two layers of I-cells. *C* and *F* show three-dimensional rendering of individual H- and I-cells. p, palisade mesophyll; s, spongy mesophyll. *A*, *Viburnum molle*. *B*, *Viburnum awabuki*. *C*, *Viburnum acerifolium*. *D*, *Viburnum punctatum*. *E*, *Viburnum davidii*. *F*, *Viburnum lantana*. Cross section: scale bars = 100 μm (× 200). Three-dimensional cells: height = 33.5 μm (*V. acerifolium*; *C*), 51.5 μm (*V. lantana*; *F*).

cut from different fixed leaves for each species between second-order veins close to the middle of the lamina. The sections were dehydrated through an ethanol series (Ruzin 1999), then infiltrated and embedded in glycol methacrylate (JB-4 Plus embedding kit; Polysciences). The embedded leaf tissue was then cross-sectioned in the transverse plane at 5 μm with a Spencer 820 rotary microtome (American Optical). Sections were stained with a saturated solution of cresyl violet acetate in 15% ethanol, and prepared slides were observed with a Nikon Eclipse E600 (Nikon, Melville, NY) compound light microscope linked to a Nikon DXM1200C digital camera. From the digital images, the palisade type was determined as H-palisade (composed of H-cells) or I-palisade (composed of I-cells) and as being either one layer (H1, I1) or two layers (H2, I2) thick. In addition, multiple anatomical parameters were measured: the thickness of the whole leaf and of the palisade mesophyll and spongy mesophyll layers; the length, width, and perimeter of cells from the palisade and spongy mesophyll layers (20 cells from each layer); and the percentage of intercellular air space in each layer, using image analysis software (ImageJ 1.47d; National Institutes of Health).

Confocal Microscopy

Six species were selected to further characterize each type of palisade cell. With leaf transverse cross sections, only a limited two-dimensional view of the cells can be obtained. Confocal microscopy provides a three-dimensional view of the cells, allowing the visualization of the complete structure of the H-cells and I-cells. For each species (H cells: *Viburnum furcatum*, *Viburnum acerifolium*, *Viburnum lobophyllum*; I cells: *Viburnum cassinoides*, *Viburnum prunifolium*, *Viburnum lantana*), two leaf sections were collected, as previously described. The sections were cleared in a 10% NaOH solution in an oven at 42°C. They were then washed with water, dehydrated through an ethanol series, and stained with a 1% safranin O in 95% ethanol solution. The excess of stain was then removed using a 95% ethanol solution. The segments were then transferred to a 1 : 1 glycerol : water solution. The palisade cell types were viewed using a Zeiss LSM 510 Meta Confocal module with a Zeiss Axiovert 200M inverted microscope (Carl Zeiss Microscopy, Thornwood, NY), using a 488-nm laser for excitation. Images were taken every 0.5 μm, from the adaxial epidermis to the top of the spongy mesophyll. For each species, six individual cells were reconstructed in 3D, using the plugin TrakEM2 (Cardona et al. 2012) from the imaging software Fiji 1.47d (National Institutes of Health; Schindelin et al. 2012), and their volume and surface area were measured.

Model for Estimating Mesophyll Cell Surface Area for CO_2 Assimilation

On the basis of the approach described by Sack et al. (2013), we calculated the surface area of mesophyll cells per leaf area (A_{mes}/A), a measure of the cell surface area available for CO_2

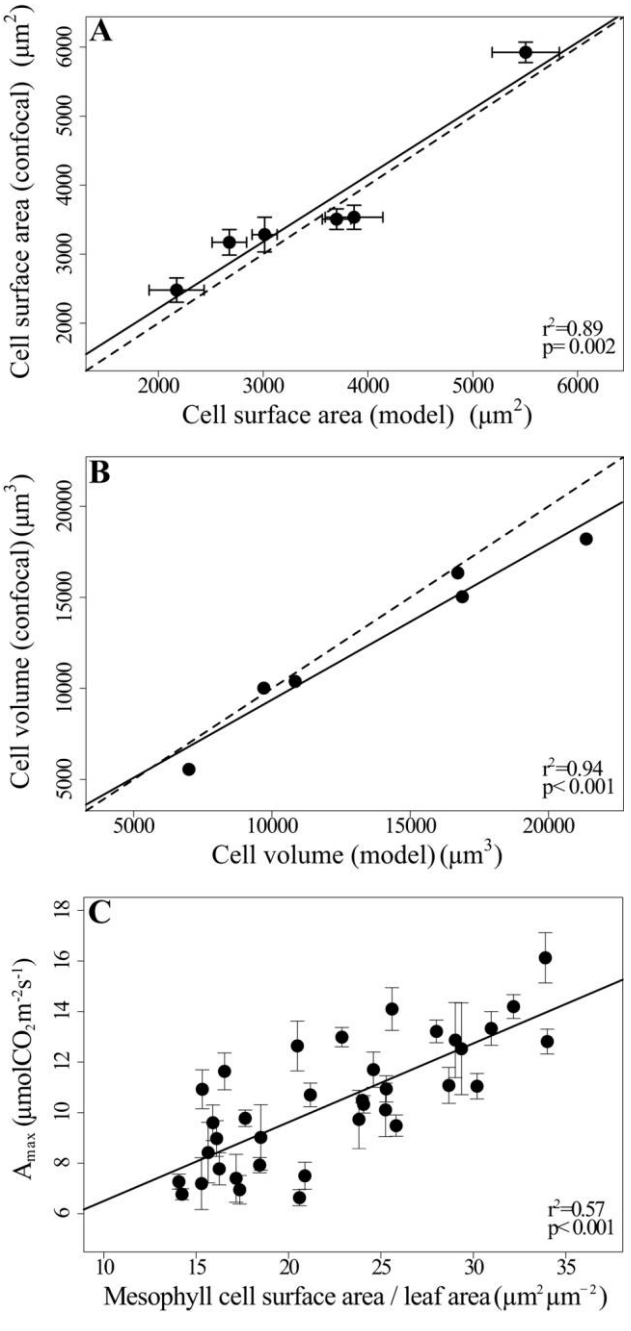

Fig. 2 Leaf anatomy–based model of photosynthetic capacity (A_{max}). Comparison between cell surface area (*A*) and cell volume (*B*) calculated with the model and measured from confocal microscopy. *C*, Correlation between A_{max} measured from 90 individuals representing 36 terminal taxa and the proxy for A_{max} calculated with the model: mesophyll cell surface area/leaf area (A_{mes}/A; average ± SE).

uptake relative to leaf area for the adaxial and abaxial mesophyll cell layers (Nobel 2009). The A_{mes}/A should correlate with maximum photosynthetic capacity across species if there is low variation in the biochemical parameters of photosynthesis and chloroplast numbers and packing or if these other determinants of photosynthesis themselves correlate with A_{mes}/A across species (Nobel et al. 1975; Longstreth et al. 1980; Nobel and Walker 1985; Patton and Jones 1989; Terashima et al. 2011; Tosens et al. 2012). Using leaf cross sections, we modeled spongy mesophyll cells as spheres, palisade I-cells as capsules, and palisade H-cells as a horizontal cylinder with arms projecting from the top and bottom. The arms were modeled as small cylinders with hemispheric caps. The total mesophyll surface area was calculated by multiplying the surface area of a given mesophyll cell by the number of cells, which in turn was estimated as the volume of mesophyll minus the air space divided by the volume of a mesophyll cell. Thus, for spongy mesophyll,

$$A_{\mathrm{mes,s}} = 4\pi\left(\frac{P_{\mathrm{sc}}}{2\pi}\right)^2 \times \frac{V_{\mathrm{st}} \times (1 - \mathrm{ASF_{st}})}{(4/3)\pi(P_{\mathrm{sc}}/2\pi)^3}, \quad (1)$$

where P_{sc} is the mesophyll cell perimeter, ASF_{st} is the spongy mesophyll intercellular air space fraction, and V_{st} is the mesophyll volume in the whole leaf (unmeasured). Because the mesophyll tissue thickness (T_{st}) is equal to the mesophyll tissue volume divided by leaf area (unmeasured), dividing both sides of the equation by leaf area and simplifying gives

$$\frac{A_{\mathrm{mes,s}}}{A} = 6\pi \times \frac{T_{\mathrm{st}} \times (1 - \mathrm{ASF_{st}})}{P_{\mathrm{sc}}}. \quad (2)$$

Similarly, for the I-cells of palisade mesophyll,

$$A_{\mathrm{mes,pic}} = 2\pi\left(\frac{D_{\mathrm{pic}}}{2}\right) \times H_{\mathrm{pic}} \times \frac{V_{\mathrm{pt}} \times (1 - \mathrm{ASF_{pt}})}{\pi(D_{\mathrm{pic}}/2)^2 \times [(4/3) \times (D_{\mathrm{pic}}/2) + H_{\mathrm{pic}} - D_{\mathrm{pic}})]}, \quad (3)$$

where D_{pic} and H_{pic} are the diameter and the height of the I-cell, V_{pt} is the palisade mesophyll volume in the whole leaf (unmeasured), and ASF_{pt} the palisade mesophyll air space fraction. Simplifying gives

$$\frac{A_{\mathrm{mes,pic}}}{A} = 2H_{\mathrm{pic}} \times \frac{T_{\mathrm{pt}} \times (1 - \mathrm{ASF_{pt}})}{(D_{\mathrm{pic}}/2) \times [(4/3) \times (D_{\mathrm{pic}}/2) + H_{\mathrm{pic}} - D_{\mathrm{pic}}]}, \quad (4)$$

where T_{pt} is the palisade thickness.

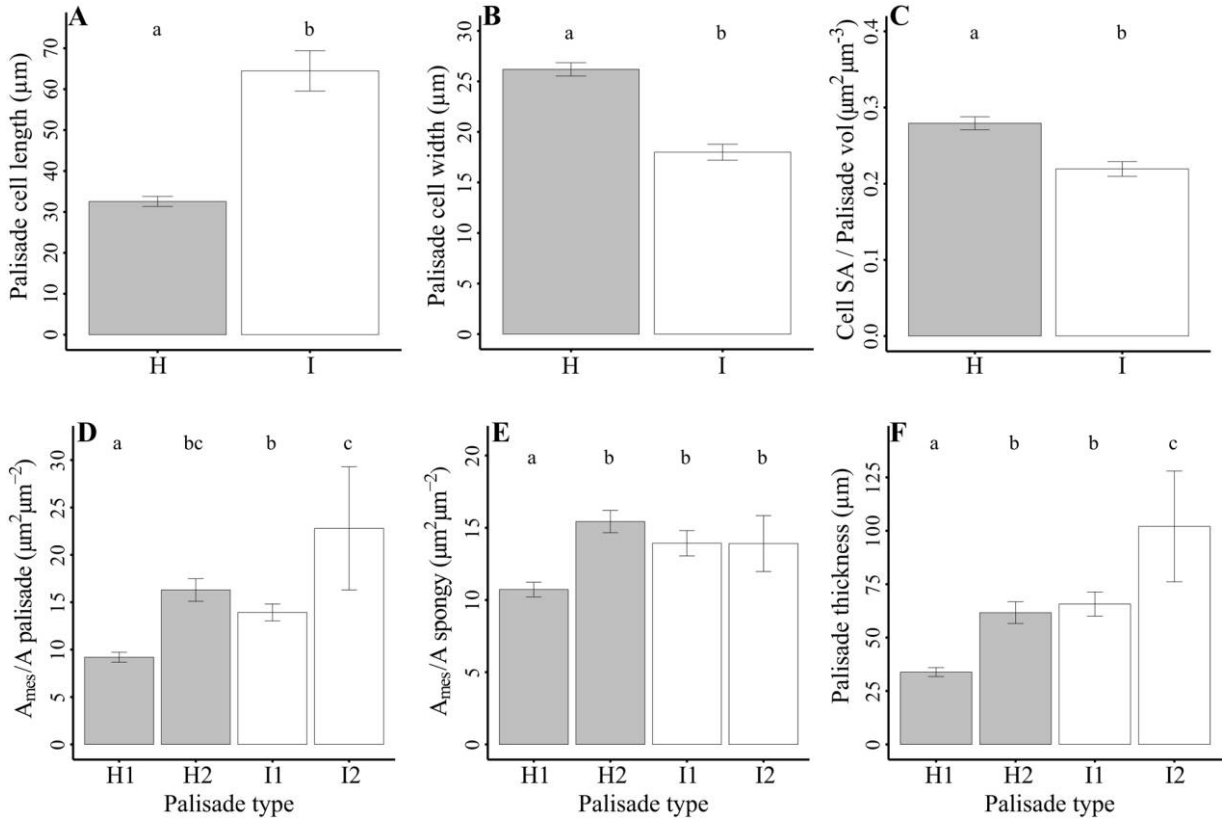

Fig. 3 Box plots of palisade cell length (*A*), palisade cell width (*B*), palisade cell surface area (SA) per palisade volume (vol; *C*), palisade cell wall surface area per leaf area (A_{mes}/A palisade; *D*), spongy cell wall surface area per leaf area (A_{mes}/A spongy; *E*), and palisade thickness (*F*) in relation to palisade type.

Similarly, for the H-cells of the palisade mesophyll,

$$A_{\text{mes, phc}} = 2\pi\frac{D_{\text{phc,c}}}{2}\left(\frac{D_{\text{phc,c}}}{2} + H_{\text{phc,c}}\right) + \sum_{i=1}^{j}\left[2\pi\frac{D_{\text{phc,arm},i}}{2} \times H_{\text{phc,arm},i} + 3\pi\left(\frac{D_{\text{phc,arm},i}}{2}\right)^2 - 2\pi\left(\frac{D_{\text{phc,arm},i}}{2}\right)^2\right] \times \left([V_{\text{pt}} \times (1 - \text{ASF}_{\text{pt}})]\Big/\left\{\pi\left(\frac{D_{\text{phc,c}}}{2}\right)^2 \times H_{\text{phc,c}} + \sum_{i=1}^{j}\left[\pi\left(\frac{D_{\text{phc,arm},i}}{2}\right)^2 \times H_{\text{phc,arm},i} + \frac{2}{3}\pi\left(\frac{D_{\text{phc,arm},i}}{2}\right)^3\right]\right\}\right). \quad (5)$$

Simplifying gives

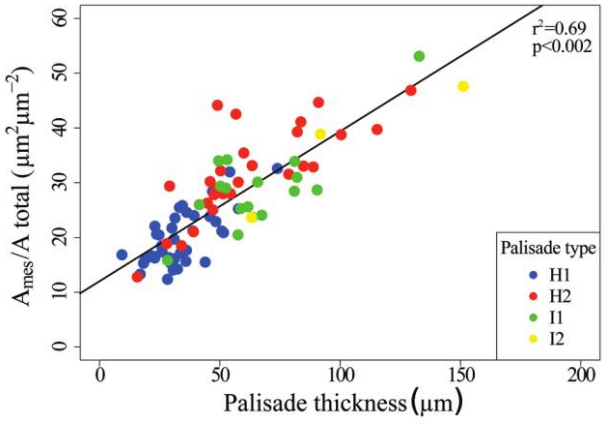

Fig. 4 Correlation between the total (palisade + spongy) mesophyll cell surface area per leaf area (A_{mes}/A total) and the palisade mesophyll layer thickness in relation to the four types of palisade: H1, H2, I1, and I2.

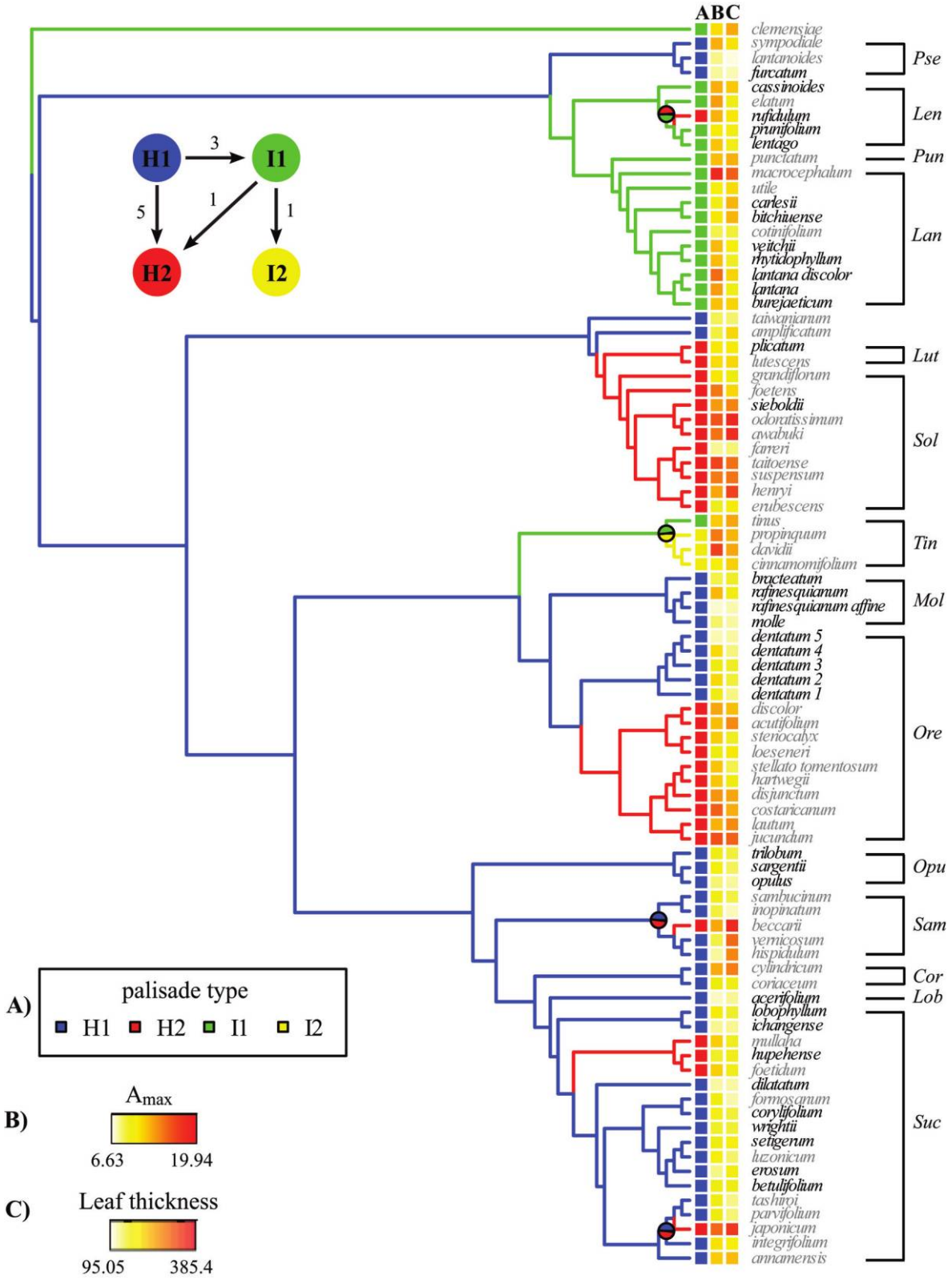

Fig. 5 Phylogenetic distribution of palisade types (*A*), modeled photosynthetic capacity (A_{max}; *B*), and leaf thickness (*C*) on a majority-rule consensus tree for 86 *Viburnum* taxa (80 species) obtained from a Bayesian analysis of DNA sequences. The tree was rooted using *Viburnum clemensiae* on the basis of previous studies. Accession names in black indicate accessions with measured A_{max}, while accession names in gray

$$\frac{A_{\text{mes, phc}}}{A} = D_{\text{phc,c}}\left(\frac{D_{\text{phc,cc}}}{2} + H_{\text{phc,c}}\right) + \sum_{i=1}^{j}\left[D_{\text{phc,arm},i} \times H_{\text{phc,arm},i} + \left(\frac{D_{\text{phc,arm},i}}{2}\right)^2\right] \times \left([T_{\text{pt}} \times (1 - \text{ASF}_{\text{pt}})] \Big/ \left\{\left(\frac{D_{\text{phc,c}}}{2}\right)^2 \times H_{\text{phc,c}} + \sum_{i=1}^{j}\left[\left(\frac{D_{\text{phc,arm},i}}{2}\right)^2 \times H_{\text{phc,arm},i} + \frac{2}{3}\left(\frac{D_{\text{phc,arm},i}}{2}\right)^3\right]\right\}\right), \quad (6)$$

where $D_{\text{phc, c}}$ and $H_{\text{phc, c}}$ are the diameter of the central cylinder of the palisade mesophyll H-cell, $D_{\text{phc, arm, }i}$ and $H_{\text{phc, arm, }i}$ are the diameter and height of the arm i projecting from the central cylinder of the palisade mesophyll H-cell, and j is the total number of arms in the palisade mesophyll H-cell.

Statistics

Statistical analysis was performed using R. Differences in the palisade cell length, width, and cell surface area per palisade volume between the palisade types H and I were analyzed using ANOVAs followed by a Tukey honestly significant difference post hoc test. The same analyses were used to compare the differences in the palisade A_{mes}/A, spongy A_{mes}/A, and the palisade thickness between the four palisade types H1, H2, I1, and I2. A value of $P < 0.05$ was considered statistically significant for all comparisons.

Phylogenetic Comparative Analysis

For analyses of character evolution, we used the Bayesian majority-rule consensus tree reconstructed in this study (fig. B1, available online). All comparative analyses were performed in R using the packages APE, GEIGER, and OUCH, and some parsimony analyses were performed using Mesquite (ver. 2.75; Maddison and Maddison 2011). Ancestral character states at all internal nodes were inferred for discrete states using both parsimony and maximum likelihood under a Brownian motion model (Pagel 1994, 1999). To evaluate the evolutionary association of different palisade types with A_{max} and leaf thickness (continuous variables), we performed a set of sister group comparisons between clades with different palisade types, locating transitions on the phylogeny and comparing the reconstructed A_{max} and leaf thickness values for the two descendant nodes. For transitions between H1 and H2, the node value of each H2 clade was compared with their corresponding H1 sister clade. The same comparisons were made for the transitions between H1 and I1, I1 and I2, and I1 and H2.

In addition to the sister group comparisons, we also evaluated the relative fit of different evolutionary models of A_{max} and leaf thickness using the R package OUCH. We compared a Brownian motion model, which assumes that traits evolved under drift or fluctuating selection with multiple Ornstein-Uhlenbeck (OU) models that describe the evolution of traits under stabilizing selection via a constant pull toward an optimum value. Among the OU models, we tested an OU model with evolution toward a single trait optimum (OU1) and OU models with two distinct optima for alternative palisade types (OU2), either H versus I or H1 versus H2 + I1 + I2.

We also wanted to test whether particular palisade types might be associated with the tropical and temperate leaf syndromes recently described in these same *Viburnum* species by Schmerler et al. (2012). To test for correlations between palisade type, leafing habit, and forest type, we reduced the multistate characters to binary states. Palisade type was classified into two binary schemes: (1) H versus I and (2) H1 (apparently ancestral; see "Results") versus H2 + I1 + I2 (apparently derived). For leafing habit and forest type, we utilized the categories and character scorings implemented by Schmerler et al. (2012). The three leafing habits (evergreen [Ev], semideciduous [SD], and deciduous [D]) were classified into two binary schemes: (1) Ev + SD versus D and (2) Ev versus SD + D. The four forests (tropical [Tr], cloud forest [CF], warm temperate [WTe], and cold temperate [CTe]) were classified into three binary schemes: (1) Tr + CF + WTe versus CTe, (2) Tr + CF versus WTe + CTe, and (3) Tr versus CF + WTe + CTe. Correlated evolution between discrete characters was analyzed with the software BayesTraits (Pagel 1994, 1999; www.evolution.rdg.ac.uk), which computes the likelihood that the probability of a state change in one trait was dependent on the state in the other trait.

All data matrices and phylogenies used in analyses are available in the Dryad Digital Repository (http://dx.doi.org/10.5061/dryad.457f7). All new sequence data has been deposited in the National Center for Biotechnology Information (app. A), and the Bayesian consensus tree and corresponding sequence matrix have been deposited in TreeBase.

Results

The phylogeny resulting from our analyses, which includes 15 newly added species (underlined in fig. B1), is largely consistent with the results of recently published phylogenetic analyses of *Viburnum* (Clement and Donoghue 2011, 2012). Here we note several exceptions (fig. B1). (1) The present analysis recovered *Tinus* as sister to *Mollodontotinus* + *Oreinodontotinus* as opposed to being the sister of a much larger clade containing *Opulus*, *Sambucina*, *Lobata*, *Coriacea*, and *Succodontotinus* in addition to *Mollodontotinus* and *Oreinodontotinus* (fig. B1). However, we note that the support for this node is insignificant (fig. B1). (2) The *Sambucina* clade now appears as sister to *Coriacea* + *Lobata* + *Succodontotinus* (posterior probability = 1). (3) *Viburnum beccarii* appears

indicate accessions with modeled A_{max}. Clade names: Pse, Pseudotinus; Len, Lentago; Pun, Punctata; Lan, Lantana; Urc, Urceolata; Lut, Lutescentia; Sol, Solenotinus; Tin, Tinus; Mol, Mollodontotinus; Ore, Oreinodontotinus; Opu, Opulus; Sam, Sambucina; Cor, Coriacea; Lob, Lobata; Suc, Succodontotinus. Pie charts indicate uncertain nodes where likelihood estimations did not agree with parsimony. In those areas, parsimony reconstruction was preferred. Inset summarizes inferred number of shifts between palisade types from parsimony analyses.

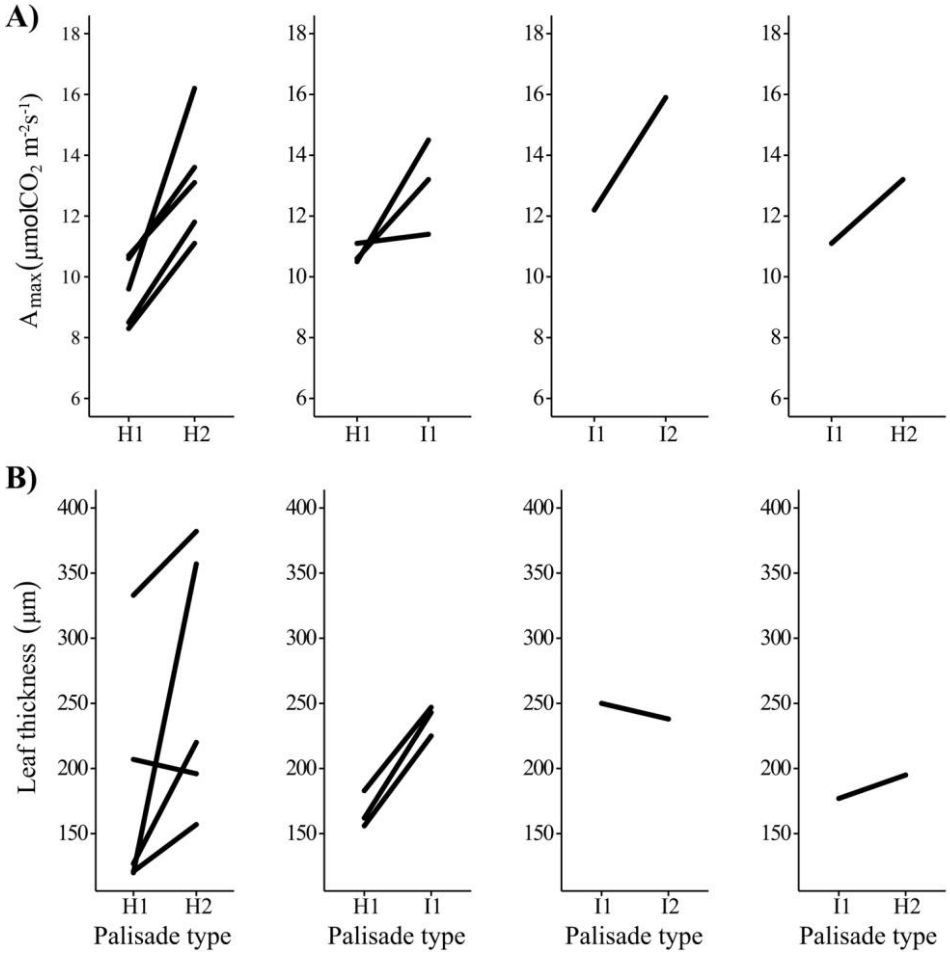

Fig. 6 Inferred transitions in photosynthetic capacity (A_{max}; *A*) and leaf thickness (*B*) reconstructed for the nodes where transitions between the different palisade types have been estimated.

within the *Sambucina* clade as opposed to within *Coriacea* (where it was placed by Kern [1951]). (4) *Viburnum amplificatum* is here resolved as sister to *Lutescentia* + *Solenotinus* as opposed to being the sister group of *Solenotinus* (Clement and Donoghue 2011). (5) The newly added *Viburnum grandiflorum* and *Viburnum foetens* appear as early diverging lineages within the *Solenotinus* clade. (6) Although the details of relationships within the Latin American species of *Oreinodontotinus* differ somewhat from previous analyses, we note that there is very little resolution and clade support in this part of the tree (fig. B1).

Leaf cross sections of 139 individuals representing our 86 *Viburnum* terminal taxa confirmed the consistent presence of palisade layers with primarily either H-cells or I-cells, with the palisade type being conserved and characteristic in a given species. More than one-third of the taxa (38/86) possess a single layer of H-cells. Others possess a single layer of I-cells (17/86) or two layers of either H-cells or I-cells (28/86 and 3/86, respectively). In cross section, the I-cells were narrow, elongated, cylindrical, and oriented perpendicular to the upper epidermis (fig. 1*D*, 1*E*). In contrast, H-cells showed one or more pairs of arms (fig. 1*A*, 1*B*) oriented radially toward the upper epidermis and/or the spongy mesophyll. Confocal microscopy revealed that H-cells have up to four to six arms on each side (fig. 1*C*).

We evaluated our geometric modeling of photosynthetic capacity in two ways. First, for six taxa, the surface area and the volume of individual cells calculated with the model were compared with values measured using confocal microscopy. Modeled cell surface area and measured cell surface area were strongly correlated ($r^2 = 0.89$, $P = 0.002$) and approached a 1 : 1 relationship (fig. 2*A*). Modeled and measured cell volumes showed an even stronger correlation ($r^2 = 0.96$, $P < 0.001$; fig. 2*B*). Second, the modeled A_{mes}/A was tested against measured A_{max} from 90 individuals representing 36 taxa measured at the Arnold Arboretum of Harvard University. The A_{max} values ranged from 6.6 to 16.1 μmol CO_2 m^{-2} s^{-1}. The measured A_{max} ($r^2 = 0.57$, $P < 0.001$) correlated well with mesophyll cell surface area per leaf area (A_{mes}/A; fig. 2*C*), which justified the use of the model to estimate A_{max} for the remaining 50 terminal taxa ($A_{max} = 0.3119 \times A_{mes}/A + 3.3818$).

We found that I-cells are significantly longer (by a factor of 2) and narrower (by a factor of 1.5) than the H-cells (fig. 3*A*, 3*B*). On a palisade volume basis, the cell wall surface area is significantly higher for H-cells than for I-cells (fig. 3*C*). On a leaf area basis, for both palisade and spongy mesophyll, H1

Table 1

Modeling the Evolution of the Photosynthetic Capacity and Leaf Thickness

	Palisade type			Habitat			Leafing habit		
Model	Group	AIC	Optima	Group	AIC	Optima	Group	AIC	Optima
A_{max}:									
B	...	465.12	...	...	465.12	...	...	978.45	...
OU	...	427.89	11.5	...	427.89	11.56	...	956.91	11.5
OU2	H1 vs. H2 + I1 + I2	<u>396.51</u>	9.0/13.0	CTe vs. WTe + CF + Tr	<u>426.51</u>	10.3/12.9	D vs. SD + Ev	<u>941.61</u>	9.9/13.1
Leaf thickness:									
B	...	978.45	...	...	978.45	...	...	465.12	...
OU	...	956.91	205.6	...	956.91	205.6	...	427.89	205.6
OU2	H1 vs. H2 + I1 + I2	<u>950.84</u>	152.3/259.2	CTe vs. WTe + CF + Tr	<u>949.11</u>	170.9/275.1	D vs. SD + Ev	<u>421.74</u>	155.1/270.9

Note. Best model determined by likelihood ratio tests and Akaike Information Criterion (AIC). Model: B, Brownian; OU, Ornstein-Uhlenbeck with 1 optimum; OU2, best OU model with different optima for two groups. Group: palisade type, H1 versus H2 + I1 + I2; habitat, cold temperate (CTe) versus warm temperate (WTe) + cloud forest (CF) + tropical (Tr); leafing habit, deciduous (D) versus semideciduous (SD) + evergreen (Ev). Best-chosen models are underlined.

leaves had significantly less cell wall surface area than the other types (fig. 3*D*, 3*E*). H2 palisade did not differ significantly from I1 and I2 palisades. Variation in the total mesophyll (palisade + spongy) cell wall surface area per leaf area (A_{mes}/A) is better explained by the palisade cell wall surface area per leaf area ($r^2 = 0.77$) than by the spongy cell wall surface area per leaf area ($r^2 = 0.54$). The palisade thickness gradually increased from H1 to I2 leaves, with H1 palisade being significantly thinner and I2 significantly thicker (fig. 3*F*). H2 and I1 palisades had similar thickness. The A_{mes}/A (palisade + spongy) is well correlated with palisade thickness ($r^2 = 0.69$, $P < 0.002$), with leaves with a thicker palisade showing a higher cell wall surface area per leaf area (fig. 4).

Mapping the four types of palisade onto our phylogeny using parsimony (fig. 5*A*) revealed 10 transitions. The inferred ancestral condition in *Viburnum* was one layer of H-cells, with five transitions to a double layer of H-palisade (H2) and three transitions to the typical single layer of elongated cells (I1). One transition was inferred from I1 to I2 and one from I1 to H2. The maximum likelihood inference generally agreed with parsimony but also inferred three possible reversions: two from H2 to H1 and one from H2 to I1. However, the likelihoods at these and neighboring nodes were highly uncertain, and we currently favor the parsimonious reconstruction.

Inferring A_{max} from our A_{mes}/A model allowed us to investigate changes in photosynthetic capacity across all 86 taxa. The A_{max} ranged from 6.6 to 19.9 μmol CO_2 m^{-2} s^{-1} (fig. 5*B*) and correlated positively with leaf thickness (fig. 5*C*; $r^2 = 0.47$). Species with lower A_{max} typically had H1 palisade. Most of the evolutionary transitions from H1 to other palisade types resulted in an increase in A_{max} and leaf thickness (fig. 6*A*, 6*B*). H2 lineages had on average 27% higher A_{max} and 61% thicker leaves than their H1 relatives. For shifts from H1 to I1, the average increases in A_{max} and leaf thickness was 21% and 42%, respectively. Surprisingly, the single shift inferred from one to two layers of I-cells was accompanied by a decrease in leaf thickness (4%) as a result of shorter I-cells and a thinner spongy mesophyll, though it did provide a slight increase in A_{max} (4%). The single transition from I1 to H2 resulted in an increase in A_{max} (18%) and leaf thickness (10%).

While palisade type correlated well with leaf thickness and photosynthetic function, we found no evidence of any relationship between this suite of traits and species habitat (tropical, cloud forest, warm temperate, cold temperate) or leaf habit (evergreen, semideciduous, deciduous; $P > 0.05$ in all cases). Species habitat was significantly correlated with leaf habit, as already shown by Schmerler et al. (2012). For all three discrete characters (palisade type, habitat, and leafing habit), the best-fitting evolutionary model for A_{max} and leaf thickness was the two-optimum OU model (table 1). The evolution of H2, I1, and I2 all correlated with higher optimal values for both A_{max} and leaf thickness.

Discussion

We have documented a diversity of palisade forms in *Viburnum* arising from multiple evolutionary shifts between these forms on a tree including 86 terminal taxa. Although a minimum of 10 shifts have occurred among the four types, the major clades tend to be characterized by one palisade form or another. This is especially true with respect to the evolutionarily derived forms. For example, I1-palisade is conserved within the large *Valvatotinus* clade that includes the *Lentago*, *Punctata*, and *Lantana* groups, with only the exception of *Viburnum rufidulum*. Likewise, I1 or I2 forms are found in the *Tinus* clade, and H2-palisade characterizes the *Lutescentia* + *Solenotinus* clade in Asia and the Latin American clade within *Oreinodontotinus*. Multiple shifts between palisade types enabled us to explore correlations with other potentially relevant attributes. It does not appear that *Viburnum* shifted in palisade type during movements between tropical and temperate biomes, and there is also no apparent relationship between palisade type and deciduous or evergreen leaf habits. Palisade anatomy therefore appears to be evolving independently of the strong temperate-tropical axis of leaf variation in *Viburnum* recently documented by Schmerler et al. (2012). On the other hand, we have found significant correlations with leaf thickness and photosynthetic capacity that partially explain the functional differences between H-cells and I-cells.

The evolutionarily derived I-cells are, on average, 1.5 times narrower than the H-cells and are around twice as long. The marked increase in the length of I-cells accounts for the generally thicker palisade layer in leaves with I1-palisade. On average, I1-palisade has 1.5 times more cell wall surface area per leaf area than H1-palisade, so chloroplasts in I-palisade have more cell wall per unit area to line up against, increasing their exposure to CO_2 and resulting in a higher A_{mes}/A in I1-palisade as compared with H1-palisade. The evolution of a second layer of H-cells yielded a comparable increase in A_{mes}/A. Because the addition of a layer of H-cells also increases palisade thickness, it would appear that increased palisade thickness itself—whether achieved through the evolution of elongate I-cells or by the addition of a layer of H-cells—is directly related to photosynthetic capacity in *Viburnum* (fig. 4).

If the evolution of either I-cells or two layers of H-cells yields functionally equivalent outcomes with respect to photosynthetic capacity, why was one solution realized in some lineages and the alternative solution in others? One possibility is that this reflects the relative ease of achieving these different morphologies in different lineages. At the moment, we know too little about the genetic regulation and developmental processes underlying such character changes (Panteris and Galatis 2005; Kozuka et al. 2011), but it is worth noting that there are several alternative developmental scenarios for the transition from H-cells to I-cells. One possibility is that a single H-cell could yield multiple I-cells by continuing invagination and complete partitioning into separate cells. We find this model unlikely, since the dimensions of I-cells do not correspond to the individual arms of H-cells; they are far wider. We quantitatively simulated an I-palisade that would have arisen from an H1-palisade according to that scenario of continuing invagination until complete partitioning by calculating A_{mes}/A, assuming that the H-cell's central cylinder completely divides to form two complete I-cells. The A_{mes}/A of one of these I-cells was estimated to be 25.9 $\mu m^2\ \mu m^{-2}$, which is twice the average measured value for A_{mes}/A of I1-palisade (13.9 $\mu m^2\ \mu m^{-2}$; fig. 3*D*). Second, if H-cells are viewed as being in the process of cell division, we might expect to observe two nuclei in some of these cells, which we did not. Hoss and Wernicke (1995) also noted the absence of two nuclei in the H-cells of *Pinus sylvestris*. All things considered, it may be more likely that the transition from H-cells to I-cells entailed a reduced lateral expansion and repression of invagination at an early stage in cell growth. In contemplating mechanisms to increase palisade thickness, it is interesting to note that we did not encounter in *Viburnum* an obvious third alternative, which would be to simply elongate individual H-cells. This may indicate a physical constraint on the dimensions of an H-cell or important trade-offs with other cell functions.

An alternative explanation for the evolution of I-palisade in some lineages and H2-palisade in others is that although the two forms may both increase A_{mes}/A, they may differ importantly with respect to other aspects of photosynthesis. Specifically, these forms may differ with respect to the interception and transmission of irradiance, which may be at least as important as CO_2 absorption in understanding the functioning of different cell/palisade types. Studies focused on plants with typical I-palisade have shown that diffuse light and direct irradiance have different effects on photosynthetic performance, with usually a reduction of photosynthetic efficiency under diffuse irradiance (Brodersen et al. 2008). Under direct irradiance, chloroplasts near the surface of the leaf need to be protected because they can be photodamaged very quickly (Kasahara et al. 2002; Sztatelman et al. 2010). In elongate I-cells, the chloroplasts are arranged along the sides of the cells, effectively providing self-shading (Zurzycki 1955; Kirk 1983; Gorton et al. 1999). In addition, the guidance of direct irradiance provided by columnar I-cells allows chloroplasts located deeper in the palisade and in the spongy mesophyll to participate in the photosynthetic process (Osborne and Raven 1986; Vogelmann and Martin 1993; DeLucia et al. 1996; Vogelmann et al. 1996; Evans et al. 2004).

It is unclear how H-palisade—composed of either one or two layers of H-cells—would compare to I-palisade with respect to performance in diffuse or direct irradiance; experimental tests of the optical properties of these alternative palisade types are now needed. Currently, we suspect that H-cells may provide some advantages under low and diffuse irradiance. In leaves with elongated palisade cells living in low light, the chloroplasts are usually found lining the upper cell walls of the palisade to maximize exposure to light (Gorton et al. 2003; Kadota et al. 2009; Davis et al. 2011). In H-cells, the combination of a smaller length-width ratio and cell wall invaginations would extend the horizontal surface area of the cell wall close to the surface of the leaf, allowing more chloroplasts closer to the surface as compared with I-cells with more limited periclinal wall area. As a result of this increase in horizontal cell wall surface area, chloroplast self-shading would be minimized, which would also improve light absorption.

On the basis of these considerations, we hypothesize that H1-palisade was retained in *Viburnum* lineages occupying lower-light environments, such as in understory temperate forests, where the irradiance is typically diffuse and less intense, with occasional sun flecks (Smith et al. 1998; Pearcy 1990). In such environments, H-cells would allow an efficient use of diffuse irradiance. Although we currently lack any direct quantitative data on natural light environments, this seems to broadly fit the habit and distribution of viburnums with H1-palisade. For example, most species of the *Pseudotinus*, *Urceolata*, *Mollodontotinus*, *Lobata*, and *Succodontotinus* clades are understory plants in shady forest environments. We further hypothesize that shifts to I-palisade corresponded to transitions into more open, direct light environments. This hypothesis is reinforced by the study of Sack and Grubb (2002), which concluded that *Viburnum opulus* (H1) is more shade tolerant than *Viburnum tinus* (I1) or *Viburnum lantana* (I1). Most species of the *Tinus* clade (I1 and I2 species) tend to occupy low-canopy, full-sunlight environments, at least as adults (e.g., *V. tinus* in the Mediterranean climates of Europe, *Viburnum propinquum* in exposed heath vegetation in the mountains of Taiwan). Similarly, species of the *Valvatotinus* clade tend to grow in open well-lit habitats. We remain uncertain about the environmental factors driving the evolution of H2-palisade. It is currently unknown, for example, whether the environments occupied by members of the Asian *Lutescentia* + *Soleninotinus* clade correspond in some meaningful way to the Latin American cloud forest species of *Oreinodontotinus*. Regardless of habitat, it is clear that a shift to an H2 palisade corresponds

to the evolution of a thicker leaf with a higher photosynthetic capacity; perhaps these lineages evolved an H2 layer to boost photosynthetic performance and leaf longevity in a diffuse-light forest understory.

Alternatively, H-cell and I-cell function could vary in ways indirectly related to photosynthesis. *Viburnum opulus* (H1), while being more shade tolerant than *V. tinus* (I1) or *V. lantana* (I1), was also found to be the least drought tolerant (Sack and Grubb 2002). It could be that H-cells are more susceptible to deformation during leaf dehydration than I-cells, thus compromising their function. During leaf dehydration, spongy mesophyll cells collapse more than the typical, elongated palisade cells (Fellows and Boyer 1977; Colpitts and Coleman 1997), probably because of the higher proportion of intercellular air space (Búrquez 1987) as well as their complex shape and their cell wall structure and properties (Webb and Arnott 1982; Pearce and Beckett 1987). While we did not find a difference in intercellular air space between the different palisade types, the lobes of the H-cells could potentially be a weaker point in the cell wall (Webb and Arnott 1982; Panteris et al 1993; Panteris and Galatis 2005).

In summary, our analyses show multiple evolutionary transitions between the four major palisade types in *Viburnum* and that shifts from the ancestral H1-palisade to the I-palisade and H2-palisade types involved corresponding shifts in palisade/leaf thickness and in photosynthetic capacity. With regard to CO_2 absorption, I1 palisade and H2 palisade apparently represent equivalent functional strategies, and *Viburnum* has repeatedly evolved these two alternative phenotypes to build a more productive leaf. We suspect that there are important distinctions between these forms that will eventually explain why I-cells evolved in some lineages and H2 in others. A more complete understanding of the functional significance of all palisade types now requires direct experimental tests of the optical performance of these different palisade arrangements, as well as more direct information on the light environments occupied by *Viburnum* in nature and their sensitivity to drought.

Acknowledgments

We thank the Arnold Arboretum of Harvard University and the Washington Park Arboretum in Seattle for access to living *Viburnum* plants. We are grateful to numerous colleagues in Taiwan, Japan, Malaysia, and Vietnam for their assistance in conducting fieldwork, especially Kuo-Fang Chung and Jer-Ming Hu in Taiwan and Tetsukazu Yahara in Japan. Finally, we thank Pascal-Antoine Christin, Monica Arakaki, Matt Ogburn, Radika Bhaskar, Elizabeth Spriggs, Alejandro Brambila, Laura Garrison, Anastasia Rahlin, Christine Scoffoni, and Patrick Sweeney for helpful discussions and/or help in the field. This work was funded by in part by National Science Foundation grants IOS-0843231 to E. J. Edwards, IOS-0842800 to M. J. Donoghue, and IOS-0842771 to L. Sack.

Appendix A

Voucher Information and GenBank Accession Numbers

Voucher information and GenBank accession numbers (psbA-trnH, rpl32-trnL$^{(UAG)}$, ITS, trnK, matK, rbcL, ndhF, trnC-ycf6, trnS-trnG, petB-petD) for *Viburnum* species sampled. Species are grouped by clade name (Clement and Donoghue 2011; Winkworth and Donoghue 2005). Missing data are indicated by a dash, and species new to *Viburnum* phylogeny are indicated by an asterisk. For each species, the collector, collector number, and herbarium where the voucher is located is provided. Herbaria abbreviations are as follows: AA, Arnold Arboretum; K, Kew Royal Botanic Garden; MO, Missouri Botanical Garden; NY, New York Botanical Garden; WTU, University of Washington Herbarium; YU, Yale University Herbarium.

Coriacea: *V. beccarii* Gamble* (P.W. Sweeney et al., 2106, YU), KF019842, KF019863, KF019808, KF019931, KF019743, KF019786, KF019766, KF019884, KF019907, KF019822. *V. coriaceum* Blume, L. (Averyanov et al., VH3300, MO), HQ592071, HQ591881, HQ591960, HQ591792, HQ591572, HQ591717, HQ591650, HQ592125, -, HQ592001. *V. cylindricum* Buch.-Ham. ex D. Don (Boufford et al., 29342, A), AY627389, HQ591883, AY265119, AY265165, -, -, -, HQ592127, EF490269, -.

Lantana: *V. bitchiuense* Makino (David Chatelet, 1097-77A, A-living collection), JX049467, JX049477, JX049448, JX049491, JX049451, JX049471, JX049459, JX049481, JX049495, JX049509. *V. burejaeticum* Regel et Herder (K. Schmandt, "375-95A, 00223095," A), JQ805297, JQ805472, -, JQ805552, JQ805231, JX049473, JX049463, JX049486, JX049500, JX049513. *V. carlesii* Hemsl. Ex Forb. & Hemsl. (M.J. Donoghue & R.C. Winkworth, 24, YU), AY627385, HQ591873, AY265115, AY265161, HQ591566, HQ591710, HQ591645, HQ592117, HQ591823, HQ591996. *V. cotinifolium* D. Don* (M.J. Donoghue, 267, YU), KF019843, KF019864, KF019809, KF019932, KF019744, KF019787, KF019767, -, KF019908, KF019823. *V. lantana* L. (M.J. Donoghue & R.C. Winkworth, 26, YU), AY627404, HQ591902, AY265134, AY265180, HQ591595, HQ591736, HQ591667, HQ592145, EF490278, HQ592019. *V. lantana v. discolor* L. (K. Schmandt, 1294-83B, A), JQ805300, JQ805474, JX049450, JQ805554, JX049455, JQ805469, -, JX049489, JX049503, JX049516. *V. macrocephalum* Fortune (M.J. Donoghue, 101, YU), HQ592086, HQ591911, EF462984, EF490247, HQ591604, HQ591745, HQ591673, HQ592153, HQ591842, HQ592027. *V. rhytidophyllum* Hemsl. Ex Forb. & Hemsl. (M.J. Donoghue & R.C. Winkworth, 8, YU), HQ592092, HQ591925, AY265146, AY265192, HQ591618, HQ591759, HQ591685, HQ592166, HQ591850, HQ592036. *V. utile* Hemsl. (Egolf, 2336-E, cultivated plant), AY627424, HQ591945, AY265156, AY265202, HQ591638, HQ591778, HQ591698, HQ592184, EF490291, HQ592054. *V. veitchii* C.H. Wright (Bouffourd et al., 27597, A), HQ592106, HQ591946, HQ591985, HQ591817, HQ591639, HQ591779, HQ591699, -, HQ591861, HQ592055.

Lentago: *V. cassinoides* L. (Arnold Arboretum, "874-85A, 0182773", A), HQ592067, HQ591874, HQ591956, HQ591789, HQ591567, HQ591711, HQ591646, HQ592118, HQ591824, HQ591997. *V. elatum* Benth (M.J. Donoghue, 472, YU),

AY627394, HQ591887, AY265124, AY265170, HQ591578, HQ591721, -, -, EF490272, HQ592003. *V. lentago* L. (M.J. Donoghue & R.C. Winkworth, 21, YU), AY627406, HQ591905, AY265136, AY265182, HQ591598, HQ591739, HQ591670, HQ592148, EF490280, HQ592022. *V. prunifolium* L. (M.J. Donoghue & R.C. Winkworth, 13, YU), AY627413, HQ591922, AY265144, AY265190, HQ591615, HQ591756, HQ591683, HQ592163, EF490286, HQ592033. *V. rufidulum* Raf. (M.J. Donoghue & R.C. Winkworth, 14, YU), AY627415 , HQ591927, AY265147, AY265193, HQ591620, HQ591761, HQ591687, HQ592167, EF490287, HQ592038.

Lobata: *V. acerifolium* L. (M.J. Donoghue & R.C. Winkworth, 27, YU), AY627384, HQ591863, AY265114, AY265160, HQ591557, HQ591701, HQ591641, HQ592108, HQ591819, HQ591987.

Lutescentia: *V. lutescens* Blume ("Wu, Phan, Gong, Xiang, Nguyen, Nguyen," WP531, A), -, HQ591909, HQ591969, HQ591802, HQ591602, HQ591743, HQ591672, HQ592151, HQ591841, HQ592025. *V. plicatum* Thunberg (M.J. Donoghue & R.C. Winkworth, 10, YU), AY627412, HQ591920, AY265143, AY265189, HQ591613, HQ591754, HQ591681, HQ592161, EF490285, HQ592032.

Mollodontotinus: *V. bracteatum* Rehder (Arnold Arboretum, "1067-87A, 0227564," A), HQ592065, HQ591871, -, KF019933, HQ591564, HQ591708, HQ591643, HQ592115, HQ591822, HQ591994. *V. molle* Michx. (M.J. Donoghue & R.C. Winkworth, 5, YU), AY627409 , HQ591913, AY265139, AY265185, HQ591606, HQ591747, HQ591675, HQ592154, EF490281, -. *V. rafinesquianum var. affine* Schult. (David Chatelet, "4622-2B, 00184665," A), JX049470, JX049480, JX049449, JX049494, JX049454, JX049476, JX049461, JX049484, JX049498, JX049512. *V. rafinesquianum* Schult. (M.J. Donoghue & R.C. Winkworth, 4, YU), AY627414, HQ591924, AY265145, AY265191, HQ591617, HQ591758, HQ591684, HQ592165, HQ591849, HQ592035.

Opulus: *V. opulus* L. (W.L. Clement, 250, YU), -, HQ591918, HQ591972, HQ591805, HQ591611, HQ591752, HQ591679, HQ592159, HQ591847, -. *V. sargentii* Koehne (M.J. Donoghue & R.C. Winkworth, 17, YU), AY627416, HQ591928, AY265148, AY265194, HQ591621, HQ591762, HQ591688, HQ592168, EF490288, HQ592039. *V. trilobum* Marshall (Arnold Arboretum, "22900A, 0174487," AA), HQ592104, HQ591942, HQ591983, HQ591815, HQ591635, HQ591775, HQ591695, HQ592182, EF490290, HQ592051.

Oreinodontotinus: *V. acutifolium* Benth. (M.J. Donoghue, 96, YU), JQ805307, -, JQ805160, -, JQ805237, JQ805397, -, KF019885, -, -. *V. costaricanum* (Oerst.) Hemsl. (M.J. Donoghue, 85, YU), -, JQ805482, JQ805164, JQ805564, -, -, -, -, KF019909, -. *V. dentatum-1* L. (Arnold Arboretum, "18008, 00223755," A), JQ805312, JQ805484, -, -, JX049456, JQ805385, JX049464, JX049487, JX049502, JX049514. *V. dentatum-2* L. (M.J. Donoghue & R.C. Winkworth, 33, YU), AY627391, HQ591884, AY265121, AY265167, HQ591574, HQ591718, HQ591651, HQ592128, HQ591827, HQ592002. *V. dentatum-3* L (Arnold Arboretum, 1253-83C, A-living collection), JX049468, JX049478, JX049447, JX049492, JX049452, JX049474, -, JX049482, JX049496, JX049510. *V. dentatum-4* L. (Arnold Arboretum, "101-38A, 00224160," A), JQ805313, JQ805483, JQ805165, JQ805565, KF019746, JQ805386, -, JX049488, JX049501, JX049515. *V. dentatum-5* L. (Arnold Arboretum, "1471-83B, 00192902," A), JQ805337, JQ805507, JQ805189, JQ805585, JQ805261, JQ805387, JX049465, JX049490, JX049504, KF019824. *V. discolor* Benth. ("M. Veliz, N. Gallardo, M. Vasquez," 35-99, MO), JQ805314, JQ805485, JQ805166, -, JQ805241, JQ805402, -, KF019886, -, -. *V. disjunctum* C.V. Morton* (M.J. Donoghue, 700, YU), KF019844, -, KF019810, -, KF019745, KF019788, -, KF019887, KF019910, -. *V. hartwegii* Benth. (M.J. Donoghue, 486, YU), AY627400, HQ591894, AY265130, AY265176, HQ591586, -, HQ591659, HQ592137, HQ591832, HQ592011. *V. jucundum* C.V. Morton (M.J. Donoghue, 244, YU), AY627402, HQ591900, AY265132, AY265178, HQ591593, HQ591734, HQ591665, -, HQ591838, HQ592017. *V. lautum* C.V. Morton (M.J. Donoghue, 72, YU), HQ592082, HQ591904, HQ591967, HQ591799, HQ591597, HQ591738, HQ591669, HQ592147, HQ591839, HQ592021. *V. loeseneri* Graebn. (M.J. Donoghue, 2547, YU), HQ592084, HQ591908, HQ591968, HQ591801, HQ591601, HQ591742, -, HQ592150, -, HQ592024. *V. stellato-tomentosum* (Oerst.) Hemsl.* (M.J. Donoghue, 640, YU), KF019845, KF019865, -, -, KF019747, KF019789, -, KF019888, KF019911, -. *V. stenocalyx* Hemsl. (M.J. Donoghue, 60, YU), HQ592097, HQ591933, HQ591978, HQ591810, HQ591626, HQ591767, -, HQ592173, KF019912, HQ592043.

Pseudotinus: *V. furcatum* Blume ex Hook.f. & Thomson (Tsugaru & Takashi, 19958, MO), AY627399 , HQ591893, AY265129, AY265175, HQ591585, HQ591728, HQ591658, HQ592136, EF490275, HQ592010. *V. lantanoides* Michx. (M.J. Donoghue & R.C. Winkworth, 2, YU), AY627405, HQ591903, AY265135, AY265181, HQ591596, HQ591737, HQ591668, HQ592146, EF490279, HQ592020. *V. sympodiale* Graebn. (Lai & Shan, 4529, MO), HQ592100, HQ591937, EF462988, EF490252, HQ591630, HQ591770, -, HQ592177, EF490289, HQ592046.

Punctata: *V. punctatum* Buch.-Ham. Ex D. Don (P.W. Sweeney et al., 2097, YU), -, KF019866, -, KF019934, KF019748, KF019790, KF019768, KF019889, KF019913, KF019825.

Sambucina: *V. hispidulum* J. Kern* (P.W. Sweeney et al., 2136, YU), KF019846, KF019867, -, KF019935, KF019749, KF019791, KF019769, KF019890, KF019914, KF019826. *V. inopinatum* Craib. (P.W. Sweeney et al., 2091, YU), KF019847, KF019868, -, KF019936, KF019750, KF019792, KF019770, KF019891, KF019915, KF019827. *V. sambucinum* Reinw. Ex Blume* (P.W. Sweeney et al., 2100, YU), KF019848, KF019869, KF019811, KF019937, KF019751, KF019793, KF019771, KF019892, KF019916, KF019828. *V. vernicosum* Gibbs* (P.W. Sweeney et al., 2123, YU), KF019849, KF019870, KF019812, KF019938, KF019752, KF019794, KF019772, KF019893, KF019917, KF019829.

Solenotinus: *V. awabuki* Hort.Berol. Ex K. Koch (Liu, 141, A), HQ592060, HQ591867, HQ591951, HQ591783, HQ591560, HQ591704, -, HQ592111, -, HQ591990. *V. erubescens* Wall. (Boufford et al., 27190, A), AY627397, HQ591889, AY265127, AY265173, HQ591581, HQ591724, HQ591655, HQ592133, HQ591831, HQ592006. *V. farreri* Stearn (M.J. Donoghue &

R.C. Winkworth, 18, YU), AY627398, HQ591890, AY265128, AY265174, HQ591582, HQ591725, HQ591656, HQ592134, EF490274, HQ502007. *V. foetens* Decne.* (M.J. Donoghue, 270, YU), KF019851, KF019872, KF019813, KF019940, KF019754, KF019796, KF019774, KF019895, KF019919, KF019831. *V. grandiflorum* Wall. Ex DC* (M.J. Donoghue, 271, YU), KF019852, KF019873, KF019814, KF019941, KF019755, KF019797, KF019775, KF019896, KF019920, KF019832. *V. henryi* Hemsl.* (M.J. Donoghue, 272, YU), KF019853, KF019874, KF019815, KF019942, KF019756, KF019798, KF019776, KF019897, KF019921, -. *V. odoratissimum* Ker-Gawl. (R. Olmstead, 118, WTU), AY627411, HQ591916, AY265141, AY265187, HQ591609, HQ591750, HQ591678, HQ592157, HQ591845, -. *V. sieboldii* Miq. (M.J. Donoghue & R.C. Winkworth, 3, YU), AY627417, HQ591932, AY265149, AY265195, HQ591625, HQ591766, HQ591691, HQ592172, HQ591853, HQ592042. *V. suspensum* Lindl. (M.J. Donoghue & R.C. Winkworth, 36, YU), AY627419, HQ591936, AY265151, AY265197, HQ591629, HQ591769, HQ591692, HQ592176, HQ591854, HQ592045. *V. taitoense* Hayata* (M.J. Donoghue and KFC, 1941, YU), KF019854, KF019875, KF019816, KF019943, KF019757, KF019799, KF019777, KF019898, KF019922, KF019833.

Succodontotinus: *V. annamensis* Fukouoka* (P.W. Sweeney et al., 2094, YU), KF019855, KF019876, -, KF019944, KF019758, KF019800, KF019778, KF019899, KF019923, KF019834. *V. betulifolium* Batalin ("Boufford, Bartholomew, Chen, Donoghue, Ree, Sun, Wu," 29335, A), HQ592061, HQ591868, -, HQ591784, HQ591561, HQ591705, -, HQ592112, -, HQ591991. *V. cf. corylifolium* Hook.f. & Thomson (David Chatelet, 103-99A, A), JX049469, JX049479, KF019817, JX049493, JX049453, JX049475, JX049460, JX049483, JX049497, JX049511. *V. dilatatum* Thunberg (M.J. Donoghue & R.C. Winkworth, 19, YU), AY627392, HQ591885, AY265122, AY265168, HQ591575, HQ591719, HQ591652, HQ592129, HQ591828, -. *V. erosum* Thunberg (M.J. Donoghue & R.C. Winkworth, 16, YU), AY627396, HQ591888, AY265126, AY165172, HQ591580, HQ591723, HQ591654, HQ592132, EF490273, HQ592005. *V. foetidum var. rectangulatum* (Graebn.) Rehder (M.J. Donoghue and KFC, 1942, YU), KF019856, KF019877, KF019818, KF019945, KF019759, KF019801, KF019779, KF019900, KF019924, KF019835. *V. formosanum* Hayata* (M.J. Donoghue and JM Hu, 2007, YU), KF019857, KF019878, -, KF019946, KF019760, KF019802, KF019780, KF019901, KF019925, KF019836. *V. hupehense* Rehder (Bartholomew et al., 1286, A), HQ592077, HQ591896, HQ591964, HQ591796, HQ591588, HQ591730, HQ591661, HQ592139, HQ591834, HQ592013. *V. ichangense* Rehder (Bartholomew et al., 1889, A), HQ592078, HQ591897, HQ591965, HQ591797, HQ591589, HQ591731, HQ591662, HQ592140, HQ591835, HQ592014. *V. integrifolium* Hayata (M.J. Donoghue and KFC, 1946, YU), KF019858, KF019879, -, KF019947, KF019761, KF019803, KF019781, KF019902, KF019926, KF019837. *V. japonicum* Spreng (NVI, s.n., YU), AY627401, HQ591899, AY265131, AY265177, HQ591592, HQ591733, HQ591664, HQ592143, HQ591837, HQ592016. *V. lobophyllum* Graebn. (M.J. Donoghue & R.C. Winkworth, 25, YU), AY627407, HQ591907, AY265137, AY265183, HQ591600, HQ591741, HQ591671, HQ592149, HQ591840, HQ592023. *V. luzonicum* Rolfe (Shen, 673, A), HQ592085, HQ591910, HQ591970, HQ591803, HQ591603, HQ591744, JX049466, HQ592152, JX049507, HQ592026. *V. mullaha* Buch.-Ham. Ex D.Don* (M.J. Donoghue, 274, YU), KF019859, KF019880, KF019819, KF019948, KF019762, KF019804, KF019782, KF019903, KF019927, KF019838. *V. parvifolium* Hayata (M.J. Donoghue and KFC, 1953, YU), KF019860, KF019881, KF019820, KF019949, KF019763, KF019805, KF019783, KF019904, KF019928, KF019839. *V. setigerum* Hance (M.J. Donoghue, 102, YU), HQ592096, HQ591931, HQ591977, EF490251, HQ591624, HQ591765, HQ591690, HQ592171, HQ591852, HQ592041. *V. tashiroi* Nakai* (M.J. Donoghue, s.n., YU), KF019861, KF019882, -, KF019950, KF019764, KF019806, KF019784, KF019905, KF019929, KF019840. *V. wrightii* Miquel (Yonekura, 1362, A), HQ592107, HQ591947, HQ591986, HQ591818, HQ591640, HQ591780, HQ591700, HQ592185, HQ591862, HQ592056.

Tinus: *V. cinnamomifolium* Rehder (Olmstead, 120, WTU), AY627386 , HQ591877, AY265116, AY265162, HQ591568, HQ591713, HQ591647, HQ592121, HQ591826, HQ591998. *V. davidii* Franchet (M.J. Donoghue, 269, YU), KF019862, KF019883, KF019821, KF019951, KF019765, KF019807, KF019785, KF019906, KF019930, KF019841. *V. propinquum* Hemsl. (M.J. Donoghue, 100, YU), HQ592090, HQ591921, EF462987, EF490250, HQ591614, HQ591755, HQ591682, HQ592162, -, -. *V. tinus* L. (M.J. Donoghue & R.C. Winkworth, 35, YU), AY627420, HQ591940, AY265152, AY265198, HQ591633, HQ591773, HQ591693, HQ592180, HQ591857, HQ592049.

Urceolata: *V. taiwanianum* Hayata (W.-H. Hu et al., 2186, MO), HQ592101, HQ591938, EF462989, EF490253, HQ591631, HQ591771, -, HQ592178, HQ591855, HQ592047.

Unassigned: *V. amplificatum* J. Kern (P.W. Sweeney et al., 2149, YU), KF019850, KF019871, -, KF019939, KF019753, KF019795, KF019773, KF019894, KF019918, KF019830. *V. clemensiae* Kern (J. Beaman, 11781, K), AY627387, HQ591878, AY265117, AY265163, HQ591569, HQ591714, HQ591648, HQ592122, EF490267, HQ591999.

Literature Cited

Brodersen CR, TC Vogelmann, WE Williams, HL Gorton 2008 A new paradigm in leaf-level photosynthesis: direct and diffuse lights are not equal. Plant Cell Environ 31:159-164.

Búrquez A 1987 Leaf thickness and water deficit in plants: a tool for field studies. J Exp Bot 38:109–114.

Campbell R 1972 Electron microscopy of the development of needles of *Pinus nigra* var. *maritima*. Ann Bot 36:711–720.

Cardona A, S Saalfeld, J Schindelin, I Arganda-CarrerasI, S Preibisch, M Longair, P Tomancak, V Hartenstein, RJ Douglas 2012 TrakEM2 software for neural circuit reconstruction. PLoS ONE 7:e38011, doi: 10.1371/journal.pone.0038011.

Chonan N 1970 Studies of the photosynthetic tissues in the leaves of cereal crops. V. Comparison of the mesophyll structure among seedling leaves of cereal crops. Proc Crop Sci Soc Jpn 39 (4):418–425.

Clement WL, MJ Donoghue 2011 Dissolution of *Viburnum* section *Megalotinus* (Adoxaceae) of Southeast Asia and its implications for

morphological evolution and biogeography. Int J Plant Sci 172:559–573.

——— 2012 Barcoding success as a function of phylogenetic relatedness in *Viburnum*, a clade of woody angiosperms. BMC Evol Biol 12:73.

Colpitts BG, WK Coleman 1997 Complex permittivity of the potato leaf during imposed drought stress. IEEE Trans Geosci Remote Sens 35:1059–1064.

Darriba D, GL Taboada, R Doallo, D Posada 2012 jModelTest 2: more models, new heuristics and parallel computing. Nat Meth 9: 772.

Davis PA, S Caylor, C Whippo, RP Hangarter 2011 Changes in leaf optical properties associated with light-dependent chloroplast movements. Plant Cell Environ 34:2047–2059.

DeLucia EH, K Nelson, TC Vogelmann, WK Smith 1996 Contribution of intercellular reflectance to photosynthesis in shade leaves. Plant Cell Environ 19:159–170.

Evans JR, TC Vogelmann, WE Williams, HL Gorton 2004 Chloroplast to leaf. Pages 107–132 *in* WK Smith, TC Voegelmann, C Critchley, eds. Photosynthetic adaptation: chloroplast to landscape. Springer, Berlin.

Fellows RJ, JS Boyer 1977 Altered ultrastructure of cells of sunflower leaves having low water potentials. Protoplasma 93:381–395.

Gorton HL, SK Herbert, TC Vogelmann 2003 Photoacoustic analysis indicates that chloroplast movement does not alter liquid-phase CO_2 diffusion in leaves of *Alocasia brisbanensis*. Plant Physiol 132:1529–1539.

Gorton HL, WE Williams, TC Vogelmann 1999 Chloroplast movement in *Alocasia macrorrhiza*. Physiol Plant 106:421–428.

Guindon S, O Gascuel 2003 A simple, fast and accurate method to estimate large phylogenies by maximum-likelihood. Syst Biol 52: 696–704.

Haberlandt G 1884 Physiologische Pflanzenanatomie. Engelmann, Leipzig.

Harris WM 1971 Ultrastructural observations on the mesophyll cells of pine leaves. Can J Bot 49:1107.

Hoss S, W Wernicke 1995 Microtubules and the establishment of apparent cell wall invaginations in mesophyll cells of *Pinus sylvestris* L. J Plant Physiol 147:474–476.

Huelsenbeck JP, FR Ronquist 2001 MrBayes: Bayesian inference of phylogeny. Biometrics 17:754–755.

Johnson DM, WK Smith, TC Vogelmann, CR Brodersen 2005 Leaf architecture and direction of incident light influence mesophyll fluorescence profiles. Am J Bot 92:1425–1431.

Kadota A, N Yamada, N Suetsugu, M Hirose, C Saito, K Shoda, S Ichikawa, T Kagawa, A Nakano, M Wada 2009 Short actin-based mechanism for light-directed chloroplast movement in *Arabidopsis*. Proc Natl Acad Sci USA 106:13106–13111.

Kasahara M, T Kagawa, K Oikawa, N Suetsugu, M Miyao, M Wada 2002 Chloroplast avoidance movement reduces photodamage in plants. Nature 420:829–832.

Kern JH 1951 The genus *Viburnum* (Caprifoliaceae) in Malaysia. Reinwardtia 1:107–170.

Kirk JTO 1983 Light and photosynthesis in aquatic ecosystems. Cambridge University Press, Cambridge.

Kozuka T, S-G Kong, M Doi, K-I Shimazaki, A Nagatani 2011 Tissue-autonomous promotion of palisade cell development by phototropin 2 in *Arabidopsis*. Plant Cell 23:3684–3695.

Longstreth DJ, TL Hartsock, PS Nobel 1980 Mesophyll cell properties for some C_3 and C_4 species with high photosynthetic rates. Physiol Plant 48:494–498.

Maddison WP, DR Maddison 2011 Mesquite: a modular system for evolutionary analysis. Version 2.75. http://mesquiteproject.org.

Meyer FJ 1962 Das tropische Parenchym. A. Assimilationsgewebe. Encyclopedia of plant anatomy. Band IV. Teil 7A. Gebrüder Borntraeger, Berlin.

Nobel PS 2009 Physicochemical and environmental plant physiology. 5th ed. Academic Press, San Diego, CA.

Nobel PS, WB Walker 1985 Structure of leaf photosynthetic tissue. Pages 501–536 *in* J Barber, NR Baker, eds. Photosynthetic mechanism and the environment. Elsevier, Amsterdam.

Nobel PS, LI Zaragoza, WK Smith 1975 Relation between mesophyll surface area, photosynthetic rate, and illumination level during development for leaves of *Plectranthus parviflorus* Henckel. Plant Physiol 55:1067–1070.

Osborne BA, JA Raven 1986 Light absorption by plants and its implications for photosynthesis. Biol Rev 61:1–61.

Pagel M 1994 Detecting correlated evolution on phylogenies: a general method for the comparative analysis of discrete characters. Proc R Soc B 255:37–45.

——— 1999 The maximum likelihood approach to reconstructing ancestral character states of discrete characters on phylogenies. Syst Biol 48:612–622.

Panteris E, P Apostolakos, B Galatis 1993 Microtubule organization and cell morphogenesis in two semi-lobed cell types of *Adiantum capillus-veneris* L. leaflets. New Phytol 125:509–520.

Panteris E, B Galatis 2005 The morphogenesis of lobed plant cells in the mesophyll and epidermis: organization and distinct roles of cortical microtubules and actin filaments. New Phytol 167:721–731.

Patton L, MB Jones 1989 Some relationships between leaf anatomy and photosynthetic characteristics of willows. New Phytol 111:657–661.

Pearce RS, A Beckett 1987 Cell shape in leaves of drought-stressed barley examined by low temperature scanning electron microscopy. Ann Bot 59:191–195.

Pearcy RW 1990 Sunflecks and photosynthesis in plant canopies. Ann Rev Plant Physiol Plant Mol Biol 41:421–53.

Rambaut A, AJ Drummond 2007 Tracer. Version 1.5. http://beast.bio.ed.ac.uk/software/tracer.

Reinhard MO 1905 Die Membranfalten in den Pinus-Nadeln. Bot Zeitung 63:29.

Ruzin SE 1999 Plant microtechnique and microscopy. Oxford University Press, New York.

Sack L, DS Chatelet, C Scoffoni, PrometheusWiki contributors 2013 Estimating the mesophyll surface area per leaf area from leaf cell and tissue dimensions measured from transverse cross-sections. PrometheusWiki, http://prometheuswiki.publish.csiro.au/.

Sack L, PJ Grubb 2002 The combined impacts of deep shade and drought on the growth and biomass allocation of shade-tolerant wood seedlings. Oecologia 131:175–185.

Schindelin J, I Arganda-Carreras, E Frise, V Kaynig, M Longair, T Pietzsch, S Preibisch, et al 2012 Fiji: an open-source platform for biological-image analysis. Nat Meth 9:676–682.

Schmerler S, W Clement, J Beaulieu, D Chatelet, L Sack, MJ Donoghue, EJ Edwards 2012 Evolution of leaf form correlates with tropical-temperate transitions in *Viburnum* (Adoxaceae). Proc R Soc B 279:3905–3913.

Smith WK, DT Bell, KA Shepherd 1998 Associations between leaf orientation, structure and sunlight exposure in five western Australian communities. Am J Bot 84:1698–1707.

Sztatelman O, A Waloszek, AK Katarzyna Banaś, H Gabryś 2010 Photoprotective function of chloroplast avoidance movement: in vivo chlorophyll fluorescence study. J Plant Physiol 167:709–771.

Terashima I, JR Evans 1988 Effects of light and nitrogen nutrition on the organization of the photosynthetic apparatus in spinach. Plant Cell Physiol 29:143–155.

Terashima I, YT Hanba, D Tholen, Ü Niinemets 2011 Leaf functional anatomy in relation to photosynthesis. Plant Physiol 155:108–116.

Tosens T, Ü Niinemets, M Westoby, IJ Wright 2012 Anatomical basis of variation in mesophyll resistance in eastern Australia sclerophylls: news of a long and winding path. J Exp Bot 63:5105–5119.

Turrell FM 1936 The area of the internal exposed surface of dicotyledon leaves. Am J Bot 23:255–264.

Vogelmann TC, G Martin 1993 The functional significance of palisade tissue: penetration of directional versus diffuse light. Plant Cell Environ 16:65–72.

Vogelman TC, JN Nishio, WK Smith 1996 Leaves and light capture: light propagation and gradients of carbon fixation within leaves. Trends Plant Sci 1:65–70.

Webb MA, HJ Arnott 1982 Cell wall conformation in dry seeds in relation to the preservation of structural integrity during dessication. Am J Bot 69:1657–1668.

Weber MG, MJ Donoghue, WL Clement, AA Agarwal 2012 Phylogenetic and experimental tests of interactions among mutualistic plant defense traits in *Viburnum* (Adoxaceae). Am Nat 180: 450–463.

Wiebe HH, HA Al-Saadi 1976 The role of invaginations in armed mesophyll cells of pine needles. New Phytol 77:773–775.

Winkworth RC, MJ Donoghue 2005 *Viburnum* phylogeny based on combined molecular data: implications for taxonomy and biogeography. Am J Bot 92:653–666.

Zurzycki J 1955 Chloroplasts arrangement as a factor in photosynthesis. Acta Soc Bot Pol 24:27–63